Computers and Concrete, Vol. 1, No. 1 (2004) 47-60
DOI: http://dx.doi.org/10.12989/cac.2004.1.1.047

An analytical and computational study on energy dissipation along fracture process zone in concrete

Yanhua Zhao† and Shilang Xu‡

Department of Civil Engineering, Dalian University of Technology, Dalian, China

Zongjin Li‡†

Department of Civil Engineering, Hong Kong University of Science & Technology, Hong Kong, China
(Received June 17, 2003, Accepted October 9, 2003)

Abstract. The influence of the fracture process zone (FPZ) on the fracture properties is one of the hottest topics in the field of fracture mechanics for cementitious materials. Within the FPZ in front of a traction free crack, cohesive forces are distributed in accordance with the softening stress-separation constitutive relation of the material. Therefore, further crack propagation necessitates energy dissipation, which is the work done by the cohesive forces. In this paper g_f, the local fracture energy characterizing the energy consumption due to the cohesive forces, is discussed. The computational expression of g_f in the FPZ can be obtained for any stage during the material fracture process regarding the variation of FPZ, whether in terms of its length or width. G_{fa}, the average energy consumption along the crack extension region, has also been computed and discussed in this paper. The experimental results obtained from the wedge splitting tests on specimens with different initial notch ratios are employed to investigate the property of the local fracture energy g_f and the average value G_{fa} over the crack extension length. These results can be used to indicate the influence of the FPZ. Additionally, changes in the length of the FPZ during the fracture process are also studied.

Keywords: energy dissipation; fracture process zone; softening law; fracture energy.

1. Introduction

For quasibrittle materials such as concrete or toughened ceramics, it is commonly accepted that in front of a traction-free crack there exists a fracture process zone (FPZ). In cohesive-stress-based fracture models (Hillerborg 1983, 1985), the cohesive forces along the FPZ are distributed in accordance with the strain-softening constitutive relation σ-w of the material, where the cohesive force σ decreases monotonically against the crack opening displacement w. In the crack band model (CBM) (Bažant 1983), the FPZ is not treated as slit-like, but with a certain width. A large amount of energy dissipation occurs in the FPZ during fracture process, which mainly involves debonding, microcracking and frictional pull-out of grains. The work done by the cohesive forces in the FPZ

† Currently Visiting Scholar in Civil Engineering at The Hong Kong University of Science and Technology
‡ Professor
‡† Associate Professor

during crack propagation necessitates a great deal of energy. Therefore, any variation in FPZ, whether in its length or width, are directly associated with the fracture energy dissipation.

Regarding the influence of FPZ length on the fracture properties of materials, much evidence can be found in the literature. One obvious fact is the unsuccessful application of classical linear elastic fracture mechanics (LEFM) to concrete due to the neglect of the nonlinear zone that is almost entirely filled by the FPZ. After substituting the crack length a_0+a_{FPZ} instead of the original crack/notch length a_0 into the corresponding "equivalent LEFM" formula, one can obtain the stable fracture toughness (Bažant 2002, Karihaloo and Nallathambi 1990, Jeng and Shah 1985). The energy consumption within the FPZ can be interpreted as the crack extension resistance, meaning for crack further propagating, external work must be done to overcome the cohesive forces distributed along the FPZ. The *R* resistance curve (Bažant and Kazemi 1990, Robert and Li 1991) obtained from compliance method against the crack extension can be seen as the influence of the length of FPZ on the energy dissipation within the FPZ.

When determining the energy needed for crack growth, such as the fracture energy, it is often calculated as the area under the complete external load-displacement curve. One important premise behind these models (whether *R* resistance or the conventional fracture energy) is the assumption that the work done by the external load is all consumed FPZ, neglecting that dissipated outside the FPZ. With this assumption, these models predict the fracture behavior focused on the physically geometrical specimen size such as the width and height of specimens and the external mechanical feature such as the external load. The geometrically similar specimens of different sizes are used to determine the fracture energy by using the size effect law (Bažant and Kazemi 1990, Bažant 1986).

The crack propagation is actually two-dimensional: linear growth in the predicted direction and the opening perpendicular to the growth direction, expressing as the FPZ size: length and width. So the fracture energy should include these two energy consumptions. As an alternative to study the fracture behavior from the physically specimen geometries, the energy consumption can also be studied from the direct interaction between the energy consumption and FPZ size, including its length and width. The extended model (Hu 1992, 2002, Duan, *et al*. 2003) is one example of this kind. In these papers, the width influence on the energy dissipation is examined, where the local fracture energy is assumed to be distributed according to a bilinear function for simplicity and as a first approximation. In K_R resistance curve proposed by Prof. Xu and Reinhardt (1998, 1999), the crack extension resistance (in terms of stress intensity factor which can also be interpreted as the energy required for the crack extension) is expressed directly relating to the FPZ length. Also, it has been shown by experiments (Hu and Wittmann 1990, Idem 1991) that the length of the FPZ is not a constant during fracture process even if the FPZ is fully developed, thus the resulting energy consumption within this zone may vary accordingly.

The local fracture energy g_f perceived here is the fracture energy expended at a certain location (or over an infinitesimal region). In the light of FPZ length and width, the local fracture energy g_f is still a hot topic remaining to be further investigated in concrete fracture mechanics. In some reports g_f is expressed as a bilinear function along the ligament length (Duan, *et al*. 2002, Hu 2002). Its average integration value over the ligament length will in fact be the specific fracture energy G_f recommended by RILEM (1985).

This paper summarizes the investigation on the local fracture energy g_f of the FPZ as well as its average value, G_{fa}, along the ligament length, including their distribution, computation and properties. Through the analysis of the local fracture energy and the average fracture energy, it is more clearly to see how the FPZ size affects the energy consumption during the crack propagation, which is

beneficial for better understanding the fracture behavior of concrete.

2. The distribution of the local fracture energy, g_f

The widely used fracture energy, G_F, was initiated in the fictitious crack model (FCM) by Hillerborg (1983). It is the energy absorbed per unit crack area when the crack surfaces separate completely, or the equivalent amount of energy representing the crack growth resistance. It can be determined by the area under the entire stress-crack opening (σ-w) curve (Fig. 1), as given by the following integration:

$$G_F = \int_0^{w_0} \sigma dw \tag{1}$$

where w_0, the terminal point of crack opening displacement, represents the limit point beyond which no stress can be transferred; f_t is the direct tensile strength of the material. Note that G_F is used instead of G_f, because the G_f value determined by the RILEM recommended method exhibits a distinct size effect; G_F is the asymptotic value of G_f when the specimen is extremely large. From Eq. (1) and Fig. 1, one can find that for a fixed point, the energy absorption from zero displacement till a given opening width w is just the shaded area in Fig. 1. It can be obtained by integrating the product of the stresses and the corresponding small displacement dw over w, which provides

$$g_F(w) = \int_0^{w} \sigma dw \tag{2}$$

The quantity g_f is referred to henceforth as the local fracture energy, also known as the breaking energy (Bažant 1996) or the partial fracture energy (Guo, *et al.* 1999), and can be interpreted as the specific fracture energy or work required to open the crack surface by a distance of w. Note that if $w = w_0$, we obtain the fracture energy G_F in Eq. (1). It is apparent that g_f only correlates to the crack opening width w once the shape of traction-separation curve is decided.

Taking a general crack ahead of which the FPZ is fully developed into account (graphically illustrated in Fig. 2), one can give the distribution of local fracture energy over the length a_{FPZ} with the presence of FPZ, expressed as follows:

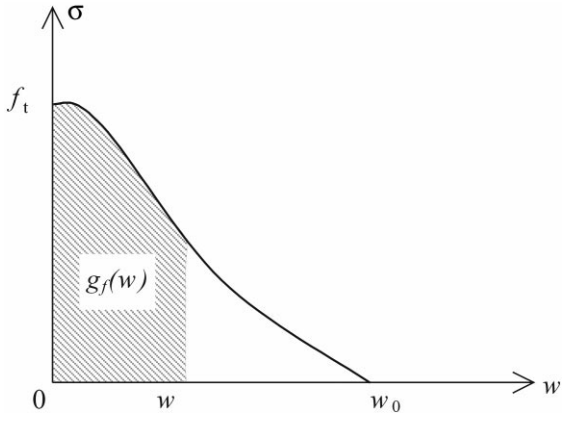

Fig. 1 The typical softening traction-separation curve

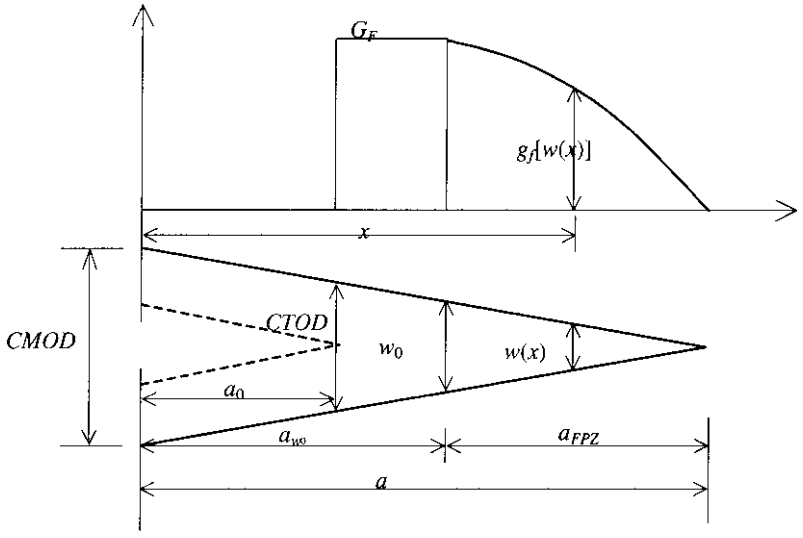

Fig. 2 The distribution of local fracture energy g_f over the crack extension span $a - a_0$

$$g_f(x) = g_f[w(x)] = \begin{cases} G_F & a_0 \le x \le a_{w_0} \\ \int_0^{w_x} \sigma[w(x)]dw & a_{w_0} \le x \le a \end{cases} \tag{3}$$

where the x coordinate is measured from the mouth of the notch; a_0 is the initial notch length; a_{w0} is the effective crack length during the crack propagation; is the intersection of these two expression where the crack opening displacement COD at this position is just equals to w_0; w_x corresponding to the crack opening width at position x; G_F represents the energy needed for a crack to open from zero to width w_0 as presented in Eq. (1).

With the above mentioned in mind, one can further get the average fracture energy, denoted as G_{fa}, along the crack extension increment $a - a_0$, which yields:

$$G_{fa}(a) = G_{f1}\gamma_1 + G_{f2}\gamma_2 = G_{f1}\frac{a_{w_0} - a_0}{a - a_0} + G_{f2}\frac{a - a_{w_0}}{a - a_0} \tag{4}$$

in which γ_1 and γ_2 are the weight function related to G_{f1} and G_{f2}, featuring respectively the contribution of G_{f1} and G_{f2} to the entire average fracture energy $G_{fa}(a)$ over the crack length increase $a - a_0$, whereas G_{f1} and G_{f2} are the average fracture energy over region $a_{w0} - a_0$ and $a - a_{w0}$, which can be calculated as

$$G_{f1} = \frac{1}{a_{w_0} - a_0}\int_{a_0}^{a_{w_0}} g_f(x)dx = G_F \tag{5}$$

$$G_{f2} = \frac{1}{a - a_{w_0}}\int_{a_{w_0}}^{a} g_f(x)dx = \frac{1}{a - a_{w_0}}\int_{a_{w_0}}^{a} [\int_0^{w_x} \sigma dw]dx \tag{6}$$

To avoid confusion, it should be noted that the meaning of local fracture energy $g_f[w(x)]$ is not

the same as the average fracture energy $G_{fa}(a)$. In fact, the local fracture energy $g_f[w(x)]$, directly derived from the tensile strain-softening relation in Fig. 1, represents the energy consumption at location x where the opening displacement varies from zero to w, while the average fracture energy $G_{fa}(a)$ is the average measurement over the crack increment $a - a_0$ when the initial crack length a_0 extends to a.

3. Analysis and computation of energy dissipation along FPZ through wedge splitting test

The wedge splitting test method, originated by Hillemeier and Hilsdorf (1977) then refined by Wittmann (Brühwileer and Wittmann 1988) in the late 1980s, proves to be a favorable test geometry to perform stable fracture tests because of its several advantages compared to other existing test methods. It is easy to be fabricated on the field or drilled form existing structures; and the calculating results will not be affected by its own weight because of the direction of load that responsible for the splitting of specimens is in the horizontal. Wedge splitting specimens also own superiority in its larger fracture area-weight ratio. Another further advantage of wedge splitting is by the use of small wedge angle, which turns a small vertical load into a relatively large horizontal one which actually responsible for the cracking of specimens, thus "artificially" reducing the requirement for the testing machine.

In this section, tests to analyze the distribution of energy dissipation throughout the FPZ were

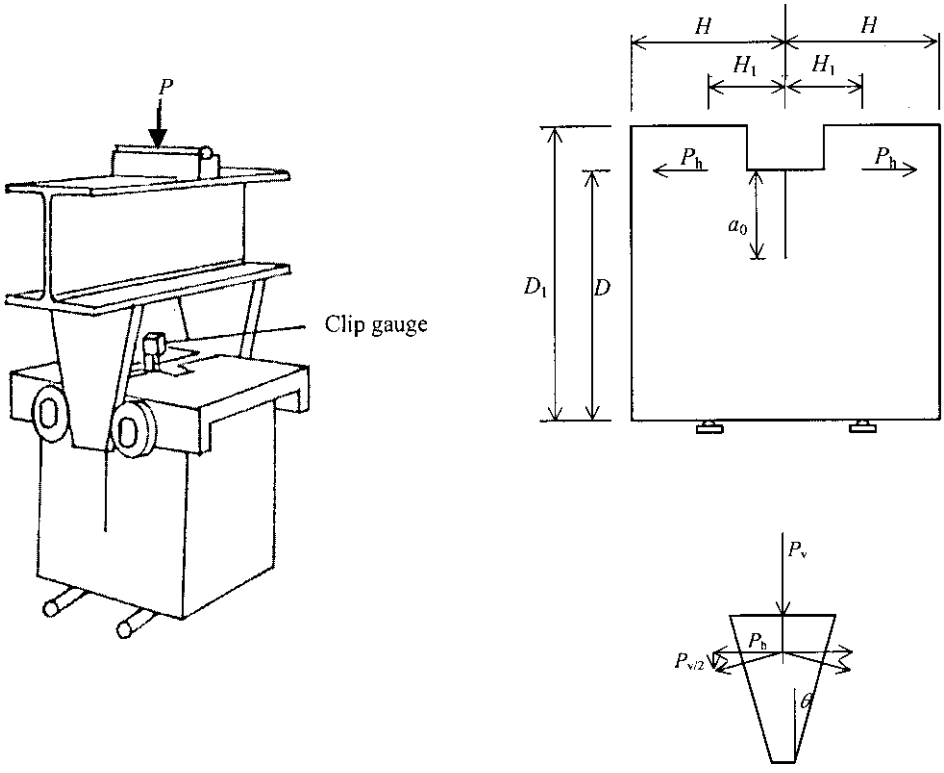

Fig. 3 The configuration of wedge splitting specimen

Table 1 The specimen dimensional and mechanical parameters

Dimension of specimen $D_1 \times 2H \times B$ (mm)	H_1 (mm)	D (mm)	Cubical compression strength f_{cu} (MPa)	f_t (MPa)	Wedge angle θ	Wedge instrument weight (kg)
200×200×200	50	170	47.96	3.182	15°	23

Table 2 Some measured experimental results

	Test serial No.	a_0/D	Elastic modulus E (GPa)
1	WS2203	0.353	35.98
	WS2303		35.58
	WS2403		40.23
2	WS904	0.471	32.94
	WS1004		30.67
	WS1104		36.17
3	WS1205	0.588	36.16
	WS1305		36.06
	WS1405		35.60
	WS1505		36.04
	WS1605		36.99
	WS1705		35.43
	WS1905		35.88
	WS2005		35.51
4	WS2506	0.706	35.74
	WS2606		35.28
	WS3106		35.70

conducted on geometrically similar notched wedge splitting concrete specimen different only in the initial relative notch length a_0/D (Fig. 3). The composite matrix was composed of Portland cement, limestone and river sand with a water-to-cement ratio of 0.56. The mix proportions are sand-to-cement of 1.94 and limestone-to-cement of 3.17, with a maximum aggregate size of 20 mm. The details of the test specimen, test procedure and experimental results have been previously reported (Zhao 2002). Here some necessary specimen dimension and mechanical parameters (Table 1) as well as some experimental results (Table 2) are listed briefly for clarity and completeness of the article. The elastic modulus E in Table 2 is calculated from the measured initial compliance of the recorded load-displacement curve through a method proposed by RILEM.

Specimens WS2203, WS1104, WS1405, and WS2506 are taken as examples to demonstrate the distribution of local fracture energy $g_f(x)$ along the FPZ as the initial crack a_0 propagates till a. To get the series effective crack length a, the set of points on the load-displacement response must be carefully chosen. Much attention will be focused on the unstable stage of crack growth, so the set of points chosen, are all equal to and beyond the maximum load.

In light of the linear asymptotic superposition assumption (Shilang and Reinhardt 1999), a complete fracture process with nonlinear features can be solved through asymptotically superimposing a series

of linear solutions obtained by the approaches of LEFM. Any point on the nonlinear load-displacement curve can be treated as a special case of the assembly of a series of linear cases. So, a solution of one point on a nonlinear load-displacement curve can be equivalently solved by the approaches of LEFM. In view of the similarity in specimen geometry and loading condition between wedge splitting and compact tension, the formula to evaluate the effective crack length for the compact tension specimen can be extended to the wedge splitting specimen (Murakami 1987)

$$COD = PV(\alpha)/BE$$

$$V(\alpha) = \left(\frac{1+\alpha}{1-\alpha}\right)^2 (2.163 + 12.219\alpha - 20.065\alpha^2 - 0.9925\alpha^3 + 20.609\alpha^4 - 9.9314\alpha^5) \quad (7)$$

where B = specimen thickness in the third dimension; D = specimen height (Fig. 3); E = material elastic modulus; $\alpha = a/D$ is the relative crack length; the above empirical equation for the relation between the load and loading line opening displacement is within 0.5 percent accuracy for $0.2 \le a \le 0.975$.

Also, it should be noted that direct experimental data (P_{vl}, $CMOD_l$) recorded from experiments must undergo some transformation before substitution into Eq. (7), that is

$$P_h = P_v/(2\text{tg}\theta) \quad (8)$$

According to Eq. (7) and Eq. (8), a values may be solved according to a linear asymptotic superposition assumption (Hu and Wittmann 1990). The next step is to compute the local fracture energy in Eq. (2). The crack opening width with $w(x)$, with coordinate x away from the crack mouth, can be captured (for simplifying reason) in a straightforward linear way featured in Fig. 2

$$w(x) = CMOD\frac{a-x}{a} \quad (9)$$

where *CMOD* is the acronym for crack mouth opening displacement. Thereafter the transition coordinate a_{w_0} may be calculated by substituting w_0 for $w(x)$ in Eq. (9). As the softening traction-separation law for concrete is used, the non-linear expression proposed by Reinhardt, *et al.* (1986) which is widely used in both numerical and analytical analyses by many researchers is employed here (sketched in Fig. 1)

$$\sigma = f_t\left\{\left[1 + \left(c_1\frac{w}{w_0}\right)^3\right]\exp\left(-c_2\frac{w}{w_0}\right) - \frac{w}{w_0}(1 + c_1^3)\exp(-c_2)\right\} \quad (10)$$

where, the coefficients c_1 and c_2 are assumed to be material constants. For normal concrete, the three parameters in Eq. (10) were determined as $c_1 = 3$, $c_2 = 6.93$, $w_0 = 160$ μm according to the testing data using a fitting process. when the shape of softening relation is determined, the local fracture energy $g_f(w)$ in Eq. (2) can be obtained by integrating Eq. (10) over the zone $0 - w$ (let $t = w/w_0$)

$$\frac{g_f(w)}{f_t w_0} = \int_0^{w/w_0}\frac{\sigma}{f_t}dt = \frac{1}{c_2}\left[1 + 6\left(\frac{c_1}{c_2}\right)^3\right] - \frac{e^{-c_2 t}}{c_2}\left[1 + c_1^3\left(t^3 + \frac{3t^2}{c_2} + \frac{6t}{c_2^2} + \frac{6}{c_2^3}\right)\right] - \frac{(1 + c_1^3)e^{-c_2 t^2}}{2} \quad (11)$$

In general, the detailed procedure to determine the distribution of the fracture energy $g_f[w(x)]$

along the FPZ for wedge splitting specimen contains the following steps:

(1) From the experimental data (P_v, *CMOD*), one can get the effective crack length a containing the FPZ according to Eq. (7) and Eq. (8) as well as some specimen dimension values;
(2) With the aid of softening traction-separation relation, the fracture energy G_F can be obtained from Eq. (11) with $t = 1$, as well as the transition crack length a_{w_0} from Eq. (9);
(3) For the local fracture energy $g_f[w(x)]$ distribution over $a–a_0$, Eq. (3) is exploited;
(4) Carry out the numerical scheme to get G_{f1} and G_{f2}, the average fracture energy over region $a_{w_0}–a_0$ and $a–a_{w_0}$ from Eq. (5) and Eq. (6), together with their respective weight function γ_1, γ_2 and the entire average fracture energy G_{fa} over $a–a_0$.

Some of the computation results are reported in Table 3. For wedge splitting specimen WS2203, WS1104, WS1405 and WS2506, the distributions of local fracture energy are illustrated in Figs. 4-7, respectively.

Table 3 Some of the computation results

Specimen No.	a_0/D	P_{vl} (KN)	$CMOD_l$ (mm)	a_{w_0}/D	a/D	a_{FPZ}/D	G_{f1} (N/m)	γ_1	G_{f2} (N/m)	γ_2	G_{fl} (N/m)
		5.74	0.0663		0.529	0.176			26.23	1.000	26.23
		4.449	0.1125		0.661	0.308			46.10	1.000	46.10
		3.424	0.1593		0.739	0.386			58.68	1.000	58.68
		1.595	0.2713		0.85	0.497			76.11	1.000	76.11
WS2203	0.353	1.545	0.2741	0.355	0.852	0.497	99.12	0.004	76.31	0.996	76.38
		1.087	0.3261	0.449	0.881	0.432	99.12	0.182	76.31	0.818	80.45
		0.718	0.4122	0.557	0.911	0.354	99.12	0.366	76.31	0.634	84.67
		0.308	0.5892	0.685	0.941	0.256	99.12	0.565	76.31	0.435	89.21
		0.103	0.8034	0.769	0.96	0.191	99.12	0.685	76.31	0.315	91.94
		3.731	0.0699		0.613	0.142	99.12		20.68	1.000	20.68
		2.2755	0.1428		0.769	0.298	99.12		47.51	1.000	47.51
		1.0045	0.2643		0.873	0.402	99.12		69.38	1.000	69.38
WS1104	0.471	0.697	0.3381	0.475	0.901	0.426	99.12	0.009	76.31	0.991	76.50
		0.4305	0.4281	0.579	0.924	0.345	99.12	0.238	76.31	0.762	81.73
		0.246	0.5574	0.672	0.943	0.271	99.12	0.426	76.31	0.574	86.04
		0.0615	0.729	0.75	0.961	0.211	99.12	0.569	76.31	0.431	89.31
		2.6445	0.0804		0.681	0.093	99.12		15.00	1.000	15.00
		2.214	0.1161		0.747	0.159	99.12		28.50	1.000	28.50
		1.189	0.2004		0.845	0.257	99.12		50.08	1.000	50.08
WS1405	0.588	0.82	0.2691		0.882	0.294	99.12		60.81	1.000	60.81
		0.265	0.433	0.589	0.934	0.345	99.12	0.003	76.31	0.997	76.37
		0.1025	0.5247	0.66	0.95	0.29	99.12	0.199	76.31	0.801	80.87
		0.0205	0.6297	0.716	0.96	0.244	99.12	0.344	76.31	0.656	84.17
		1.353	0.1044		0.782	0.076	99.12		14.01	1.000	14.01
WS2506	0.706	0.697	0.2148		0.877	0.171	99.12		40.42	1.000	40.42
		0	0.5157		0.958	0.252	99.12		72.27	1.000	72.27

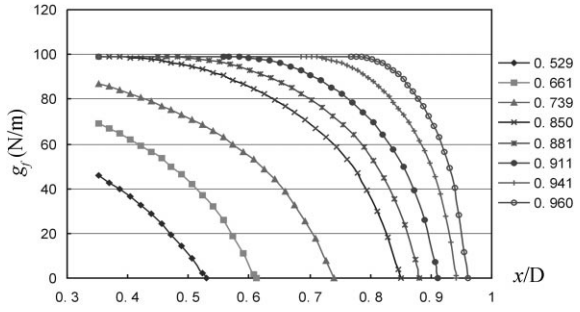

Fig. 4 The local fracture energy distribution over $(a–a_0)/D$ for specimen WS2203

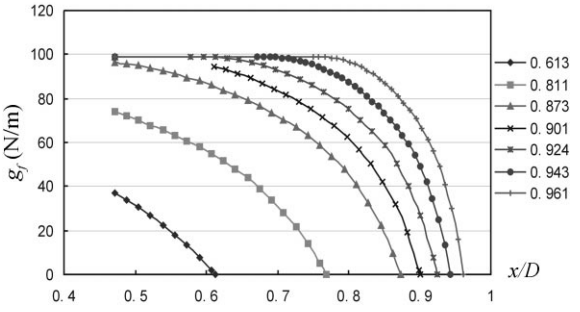

Fig. 5 The local fracture energy distribution over $(a–a_0)/D$ for specimen WS1104

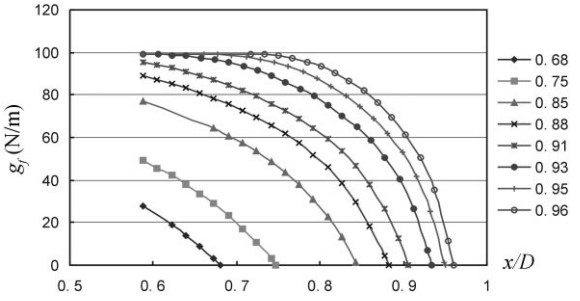

Fig. 6 The local fracture energy distribution over $(a–a_0)/D$ for specimen WS1405

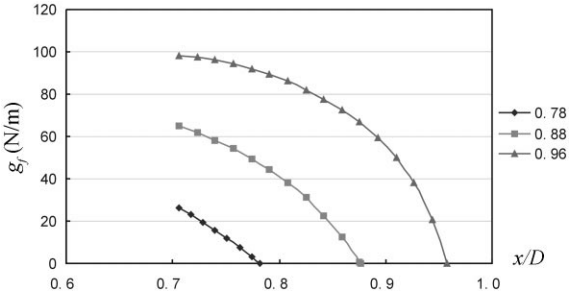

Fig. 7 The local fracture energy distribution over $(a–a_0)/D$ for specimen WS2506

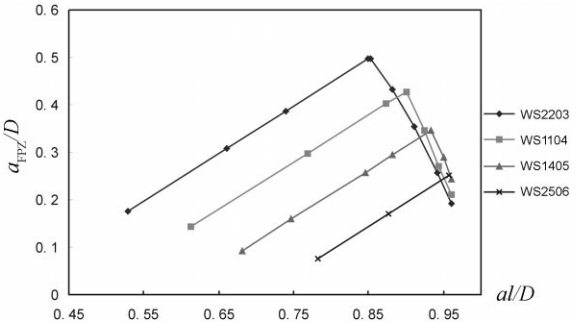

Fig. 8 The length of FPZ variation along the crack growth

4. Discussion

For specimen WS2203 with the initial crack ratio being $a_0/D = 0.353$, as an example, one can see from Fig. 4 and Table 3 that when the value a/D is less than 0.85, the FPZ is only partially developed, viz, the *CTOD* (crack tip opening displacement at $x/D = 0.353$) is less than the terminal point w_0 of the softening traction-separation curve, and the local fracture energy $g_f(x)$ distributed along the FPZ can be fitted by a second order polynomial. As the crack progresses (when the value

a/D is larger than 0.85), the FPZ varies both in length and width, guiding the change in the spread pattern of the local fracture energy. This feature can be reflected in two different expressions: the first region is the horizontal plateau with $g_f(x) = G_F$ over the range of $a_{w_0} - a_0$; while the expression for the second region $a - a_{w_0}$ shows a descending trend profile just like the case in which a/D is less than 0.85. The intersection of these two distribution lines corresponds to the crack length a_{w_0}, which is an important distinguished parameter in the computation of the entire average fracture energy G_{fa} over the entire crack $a - a_0$. As seen from Table 3 and Fig. 4, the average fracture energy G_{fa} increases proportionally more with the increase of the effective crack length a, leading to the accretion in the entire average fracture energy G_{fa}. The same thing can be said for specimens WS1104, and WS1405. However care must be taken when dealing with WS2506, because its relatively large initial crack length a_0/D is 0.706, rather close to the height of the specimen. Thus the FPZ cannot be fully developed, and only the second profile of the local fracture energy is presented. For all the specimens under consideration, the fracture become unstable before the FPZ is saturated. In the aforementioned analysis, an interesting thing that makes sense should be pointed out, that is the variation of the FPZ length a_{FPZ} when the initial crack a_0 moves forward. From Table 3, it can be found that for geometrically identical specimens, the initial crack a_0 advances in Mode I pattern, and a_{FPZ} variation falls into two apparently different stages as manifested in Fig. 8, and this phenomenon again strengthens the conclusion that the length of FPZ is not a constant even if it develops fully. The first is on the ascending branch until a_{FPZ} attaining a maximum value a^*_{FPZ}, ensuing which a somewhat steeper descending profile is met with a^*_{FPZ}, possessing some importance for better understanding the distribution of local fracture energy g_f over the crack growth quantity, corresponds to one state during the crack growth, when the *CTOD* approaches w_0 indicating the beginning of full development of FPZ. Before this state, the FPZ ahead of the traction-free crack is only partially developed, inducing small energy consumption as can be seen from Figs. 4-7. As the crack moves forward until a_{FPZ} reaches a^*_{FPZ}, the distribution of fracture energy g_f will begin to experience two different types as stated above. It should be pointed out that in this case the length of a_{FPZ} still declines along with the increase of the effective crack length a.

To justify the influence of the specimen size on the local fracture energy, the distribution of the local fracture energy over the FPZ is perceived for typical specimen WS2203, WS1104, WS1405

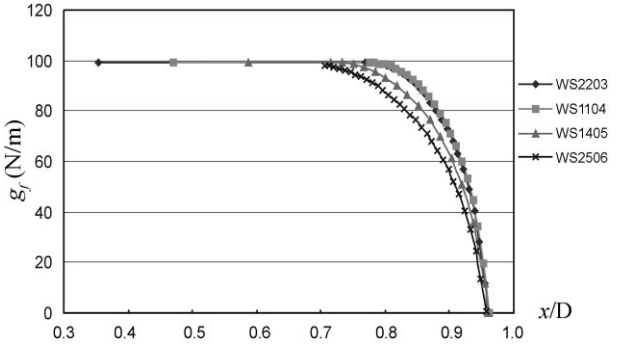

Fig. 9 The distribution of the local fracture energy at a_l/D=0.96 for wedge splitting specimen with different initial crack length

Table 4 The entire average fracture energy G_{fa} distribution of test specimens

Test serial no.	a_0/D	a_{w_0}/D	a/D	G_{fa} (N/m)
WS2203		0.769	0.96	91.94
WS2303	0.353	0.793	0.96	92.83
WS2403		0.733	0.96	90.61
Ave.				91.80
WS904		0.715	0.96	87.68
WS1004	0.471	0.775	0.961	90.45
WS1104		0.75	0.961	89.31
Ave.				89.14
WS1205		0.72	0.961	84.36
WS1305		0.714	0.96	84.01
WS1405		0.716	0.96	84.17
WS1505	0.588	0.727	0.96	84.85
WS1605		0.729	0.959	85.00
WS1705		0.717	0.96	84.21
WS1905		0.697	0.961	82.95
Ave.				82.30
WS2005		0.686	0.96	83.98
WS2506	0.706	0.661	0.958	72.27
WS2606		0.66	0.958	72.23
Ave.				70.46

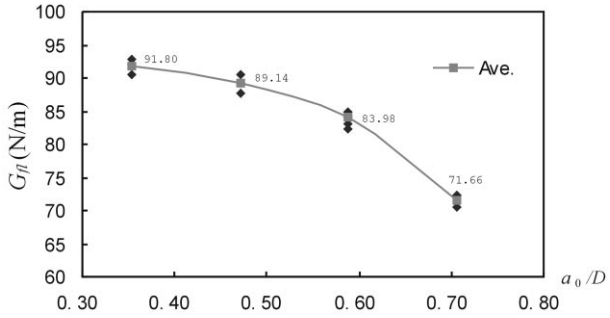

Fig. 10 The average fracture energy G_{fa} for wedge splitting specimen with different initial crack length ratio a_0/D

and WS2506 when the effective crack length is $a/D = 0.96$, approaching the height of the specimen. The plot in Fig. 9 is the computation results of local fracture energy over the entire effective crack length $a - a_0$. Obviously, specimen WS2203 with a relative longer ligament consumes more energy during the failure procedure, with the FPZ developing more fully. With a decrease in the ligament, the FPZ may not develop sufficiently, just as in specimen WS2506.

Also the average fracture energy G_{fa} over the entire effective crack length increment $a - a_0$ is

computed for all the test specimens with different initial crack ratios a_0/D, as illustrated in Table 4 and Fig. 10. In an explicit manner, the G_{fa} values decrease slowly with the increase of the initial notch a_0/D, namely G_{fa} increases with the ligament increases. The variation of FPZ, whether in length or width, can account for this phenomenon. As the ligament length shortens, the FPZ development will be confined to relatively small zone. Consequently, due to the incompletely developed distribution of FPZ which can be seen clearly in specimen WS2506, WS2606 and WS3006, the energy absorption to overcome the cohesive forces along the FPZ during the crack advances will be less.

5. Conclusions

The local fracture energy g_f and the average fracture energy G_{fa} over the crack increment is proposed in this study as an indication of the energy consumption in the region of crack extension ahead of the initial crack a_0. Their properties are associated with the FPZ development during the fracture process of concrete structures. The influence of FPZ, both in length and width, on the energy dissipation along FPZ is investigated in this paper, which yields some significant conclusions:

1. The length of FPZ, denoted by a_{FPZ}, is not a constant during the fracture process, even if it is fully developed. It increases with the propagation of the crack before attaining the critical value a^*_{FPZ}. When the *CTOD* (crack tip opening displacement) just arrives at the value w_0, then the descending branch will ensue.
2. The local fracture energy g_f, directly related to the width of the FPZ, represents the energy consumption at a certain location which can be determined according to the softening traction-separation relation. Its distribution along the crack extension is characterized by two portion after the FPZ is fully developed, the first is over the traction-free region with the value G_F; the other is over the a_{FPZ} with varying values of g_f which can be fitted by a second order polynomial. The intersection of these two distribution corresponds to the crack length a_{w_0}, where the crack opening displacement at this location is just w_0 on the softening traction-separation curve. But it should be pointed out that for a specimen in which ligament length is rather small, or the initial crack length is very close to the specimen boundary, the FPZ can not be sufficiently evolved, and the g_f will only be distributed in one form with the absence of G_F values.
3. The averaged fracture energy G_{fa} is just the average energy dissipated by the cohesive forces along the FPZ. For specimens with different initial crack length a_0, G_{fa} values decrease with increasing a_0, or in a general way we can say G_{fa} values increase with increasing ligament length. This phenomenon can be attributed to the boundary effect on the restriction of FPZ development.

Acknowledgements

This paper is supported by the National Key Basic Research and Development Program (973 Program) No. 2002CB412709. The authors also wish to thank the NSFC (Natural Science Foundation of China) for their supports (Grants No.10272068 and No.50178015). Thanks are also due to Prof. Wu Zhimin for his great help in testing procedures.

References

Bažant, Z.P. (1983), "Crack band theory for fracture of concrete, RILEM", *Materials and Structures*, **16**(93), 155-177.

Bažant, Z.P. (1986), "Determination of fracture properties from size effect tests", *J. of Structural Engineering*, ASCE, **112**(2), 289-307.

Brhwileer, E. and Wittmann, F.H. (1988), "The wedge splitting test, a method of performing stable fracture mechanics tests", *J. of Engineering Fracture Mechanics*, **5**, 117-125.

Bažant, Z.P. and Kazemi, M.T. (1990), "Determination of fracture energy, process zone length and brittleness number from size effect, with application to rock and concrete", *Int. J. of Fracture*, **44**, 111-131.

Bažant, Z.P. (1996), "Analysis of work-of-fracture method for measuring fracture energy of concrete", *J. of Engineering Mechanics*, **122**(2), 138-144.

Bažant, Z.P. (2002), "Concrete fracture models: testing and practice", *Engineering Fracture Mechanics*, **69**, 165-205.

Duan, K., Hu, X.-Z. and Wittmann, F.H. (2002), "Explanation of size effect in concrete fracture using non-uniform energy distribution", *Materials and Structures*, **35**, 326-331.

Duan, K., Hu, X.-Z. and Wittmann, F.H. (2003), "Boundary effect on concrete fracture and non-constant fracture energy distribution", *Engineering Fracture Mechanics*, **70**, 2257-2268.

Guo, X.H., Tin-Loi, F. and Li, H. (1999), "Determination of quasibrittle fracture law for cohesive crack models", *Cement and Concrete Research*, **29**, 1055-1059.

Hillerborg, A. (1983), *Analysis of One Single Crack. Fracture Mechanics of Concrete*, (edited by F.H. Wittmann), 223-249.

Hillerborg, A. (1985), "The theoretical basis of method to determine the fracture energy G_F of concrete", *Materials and Structures*, **18**(106), 291-296.

Hillemeier, B. and Hilsdorf, H.K. (1977), "Fracture mechanics studies on concrete compounds", *Cement and Concrete Research*, **7**, 523-536.

Hu, X.Z. and Wittmann, F.H. (1990), "Experimental method to determine extension of fracture process zone", *J. of Material Civil Engineering*, **2**, 15-23.

Hu, X.-Z. (1992), "Fracture energy and fracture process zone", *Materials and Structures*, **25**, 319-326.

Hu, X.-Z. (2002), "An asymptotic approach to size effect on fracture toughness and fracture energy of composite", *Engineering Fracture Mechanics*, **69**, 555-564.

Hu, X.-Z. (2002), "An asymptotic approach to size effect on fracture toughness and fracture energy of composite", *Engineering Fracture Mechanics*, **69**, 555-564.

Idem (1991), "An analytical method to determine the bridging stress transferred within the fracture process zone", *Cement and Concrete Research*, **21**, 1118-1128.

Jeng, Y.S. and Shah, S.P. (1985), "Two parameter fracture model for concrete", *J. of Engineering Mechanics, ASCE*, **111**(10), 1227-1241.

Karihaloo, B.L. and Nallathambi, P. (1990), "Effective crack model for the determination of fracture toughness K_{Ic}^{s} of concrete", **35**(4/5), 637-645.

Murakami(Editor-in-chief) (1987), *Stress Intensity Factors Handbook*. Pergamon Press, London.

Robert, Y.L. and Li, Y.-N. (1991), "Study of size effect in concrete using fictitious crack model", *J. of Engineering Mechanics*, **117**(7), 1631-1651.

Reinhardt, H.W., Cornelissen, H.A.W. and Hordijk, D.A. (1986), "Tensile tests and failure analysis of concrete", *J. of Structural Engineering*, **112**(11), 2462-2477.

RILEM-Draft-Recommandation (50-FCM) (1985), "Determination of the fracture energy of mortar and concrete by means of three-point bend tests on notched beams", *Materials and Structures*, **18**(106), 285-290.

RILEM Technical Committee 89-FMT, "Determination of fracture parameters of plain concrete using three-point bend tests, proposed by RILEM draft recommendations, RILEM", *Materials and Structures*, **23**(138), 457-460.

Shilang, X. and Reinhardt, H.W. (1998), "Crack extension resistance and fracture properties of quasi-brittle softening materials like concrete based on the complete process of fracture", *Int. J. of Fracture*, **92**, 71-99.

Shilang, X. and Reinhardt, H.W. (1999), "Crack extension resistance based on the cohesive force in concrete",

Engineering Fracture Mechanics, **64**, 563-587.
Shilang, X. and Reinhardt, H.W. (1999), "Determination of double-*K* criterion for crack propagation in quasi-brittle fracture, Part: Analytical evaluating and practical measuring methods for three-point bending notched beams", *Int. J. of Fracture*, **98**, 151-177.
Zhao Yanhua (2002), "The analytical study on the energy in the fracture process of concrete", Doctoral thesis, Dalian University of Technology.